

The bovine tubouterine junction: general organization and surface morphology

Karl-Heinz Wrobel, Richard Kujat, Gilbert Fehle

Institut für Anatomie der Universität, Universitätsstrasse 31, W-8400 Regensburg, Federal Republic of Germany

Received: 1 July 1992 / Accepted: 7 September 1992

Abstract. The bovine tubouterine junction is composed of three parts (terminal tubal segment, transition region proper, uterine apex) and follows a sigmoidal course displaying a tubal and an uterine curvature. In the terminal tubal segment, 4–8 primary longitudinal folds and a system of lower secondary folds, ridges and chords project into the centrally located lumen. The transition region proper possesses a slit-like lumen because of the existence of a thick mucosal pad containing the first uterine glands. The longitudinal primary folds of the tube broaden, flatten and start to diverge when they reach the transition region proper. The mucosal pad and broadened folds are heavily vascularized. A system of lateral outpocketings with blind ends pointing in an ampullary direction develops between the primary and secondary folds, the ridges and chords of the terminal tubal segment and transition region proper. From the bottom of these outpocketings, short tubulo-alveolar crypts originate. The mucosa of the uterine apex forms low transversal ridges. The musculature of the bovine tubouterine junction is divided into a continuous circular or spiral intermediate layer, flanked by inner and outer longitudinal layers. The outer longitudinal layer is incomplete in the terminal tubal segment but increases in thickness to form a continuous stratum in the uterine apex. An inner longitudinal layer occurs only in the terminal tubal segment where it is best developed in the bases of the primary longitudinal folds. The simple columnar surface epithelium of the tubouterine junction contains ciliated and non-ciliated cells. The former undergo cyclical changes, and increase during estrus and postestrus. During proestrus, groups of non-ciliated cells display bulbous apical protrusions. During proestrus and estrus, circumscribed epithelial lesions expose the underlying basal lamina.

Key words: Tubouterine junction – Mucosal specializations – Muscular arrangement – Microvascularization – Cyclic epithelial changes – Bovine

Correspondence to: K.-H. Wrobel

Introduction

The connection between oviduct and uterus is anatomically a highly species-specific structure. Hook and Hafez (1968) characterize four, Hafez and Black (1969) five, and Beck and Boots (1974) 10 basic patterns for the morphology of the tubouterine junction (TUJ) in mammals. According to the latter mentioned authors, the absence of an intramural oviductal segment and the lack of mucosal projections, either of oviductal or uterine origin, in the area of the juncture are typical for ruminants, such as cattle, sheep, goat, antelope and moose. At the gross-anatomical level, the uterine cornua taper off gradually toward the oviduct and a sharp flexure is present at the TUJ. Hunter et al. (1991) have depicted the pattern of folds, ridges, grooves and furrows in the bovine TUJ, and claim that these structures could provide an obstacle for ascending spermatozoa.

The existence of glands in the bovine TUJ is controversial. Lombard et al. (1950) were the first to describe gland-like structures in the isthmic portion of the tube; these have been interpreted by Hafez and Black (1969) and Hunter et al. (1991) as a continuation of uterine glands extending into the oviduct. Functionally, the TUJ has been interpreted as a sperm reservoir before ovulation (Hunter and Wilmut 1984; Larsson and Larsson 1986; Hunter et al. 1991), and as a filtering station decreasing the number of spermatozoa reaching the ampulla (Kann and Fouquet 1977).

A detailed morphological study of the bovine TUJ has revealed a number of hitherto unknown features. Here, we report the general organization, surface morphology, ciliated cell cycle and microvascularization pattern of the bovine TUJ.

Materials and methods

A total of 57 TUJ from 39 mature heifers (age 18–24 months) of the Fleckvieh breed was obtained ~15 min after slaughter. The animals were classified according to ovarian status (size and shape of corpora lutea and/or tertiary follicles), clinical evidence (appar-

ent signs of estrus, postovulatory bleeding) and serum progesterone levels, to one of the following phases of the estrus cycle, using the time schedule of Grunert (1982): estrus (day 1), postestrus (days 2–4), interestrus (days 5–15) and proestrus (days 16–21).

For light microscopy (40 TUJ), the material was fixed by vascular perfusion. A canula was inserted into the branch of the uterine artery supplying the region of the TUJ, and larger anastomoses of this vessel were ligated. Rinsing (see Wrobel et al. 1978) was performed at 25 ml/min prior to fixation. For Paraplast-embedding Bouin's solution was used as the fixative. The entire TUJ was embedded for longitudinal sectioning, whereas for cross-sectioning, the structure was divided into 3 blocks: terminal tubal segment, tubouterine transition proper and uterine apex. Serial sections were cut at a thickness of 7–10 µm and stained with Jerusalem's modification (1963) of the Masson-Goldner trichrome method.

For semithin sections, fixation was performed with solutions I and II of Forssmann et al. (1977). Selected tissue blocks from the 3 regions of the TUJ were separated and washed in 0.2 M phosphate buffer, pH 7.4. After dehydration in graded ethanols, the blocks were embedded in ERL 4206 (Spurr 1969). Semithin sections (1 µm) were stained with azur II-methylene blue or with Masson-Goldner's trichrome method.

Lectin histochemistry with GS I (*Griffonia simplicifolia*) on Paraplast-embedded material was used to visualize the complete microvascularization pattern, and was performed as described in detail by Ertl and Wrobel (1992).

Samples were prepared for scanning electron microscopy (SEM) as follows: (a) Nine complete TUJ (each of ~5 cm length) covering all phases of the estrus cycle were dissected free from serosa, in part gently flushed with fixative, opened longitudinally with scissors, spread on a flat surface, and totally immersed in fixation solution II (Forssmann et al. 1977). (b) From another 8 TUJ in the various phases of the estrus cycle, selected blocks were excised following immersion fixation as described above or perfusion fixation with the same fixative. All the fixed material was rinsed in 0.1 M phosphate buffer (pH 7.4), osmicated (1% OsO₄), washed again in buffer, and dehydrated in increasing concentrations of ethanol.

The blocks of series b were embedded in Paraplast, and characteristic locations were exposed by cutting away unwanted tissue layers by glass knives. Following removal of the Paraplast with xylene, the samples were treated like those of series a: dehydrated specimens were transferred into acetone and then subjected to critical-point drying (Anderson 1951) using liquid CO₂ substitution. The dried specimens were mounted on aluminium stubs, gold-coated in a sputter coater (Polaron) and examined and photographed in a Zeiss DSM 950 SEM.

Results

Gross anatomy of the bovine tubouterine junction (TUJ)

The TUJ consists of three parts: terminal tubal segment, transition region proper (TRP) and uterine apex (Fig. 1). The Fallopian tube displays its smallest diameter in its terminal segment. In the TRP, the duct increases continuously in thickness to reach the tip of the uterine horn. The complete TUJ follows a sigmoidal course exhibiting two curvatures. The first (tubal curvature) has its concavity at the antimesosalpingeal side, the second (uterine curvature) at the mesometrial side. Both curvatures are only exceptionally arranged in the same plane; as a rule, they overlap in a spiral-like fashion. The infundibulocornual ligament, containing longitudinally running bundles of smooth musculature, is mostly attached to the antimesosalpingeal side of the tubal curvature.

Lumen and surface morphology of the bovine TUJ

The lumen of the terminal oviducal segment is subdivided by 4–8 regularly distributed primary longitudinal mucosal folds (Figs. 5, 8) that project from the mesosalpingeal (1–2 folds), lateral (1–2 folds on each side) and antimesosalpingeal (1–2 folds) aspects of the tube. These primary longitudinal folds are interconnected by obliquely running, lower secondary folds, ridges and chords. Between all these mucosal projections, a system of shallow, slipper-shaped outpocketings with their blind ends pointing to the ovarian side can be observed (Figs. 8–15). In cross-sections, the tips of these outpocketings appear as closed rings below the level of the general lining epithelium (Figs. 8, 10, 12). Short tubulo-alveolar crypts may originate from the wall of these outpocketings (Figs. 14, 15).

The TRP connects the terminal tubal segment with the apical portion of the uterine horn. In cross-sections, the TRP possesses a slit-like, U-shaped lumen shifted excentrically to the mesometrial side, with both ends of the U pointing to the antimesometrial side (Fig. 6). The surface of the TRP is underlaid by the first true uterine glands, which are arranged nearly parallel to the long axis of the TRP, and which empty generally at very sharp angles into the lumen of the apical uterine horn (Figs. 2, 4). At the antimesometrial side of the TRP, the mucosa is considerably thicker, because it contains many more glands than does the mucosa at the opposite side (Fig. 2). Antimesometrically, the glandular layer also extends nearly to the level of the terminal tubal segment, whereas mesometrically, the glandular mucosa ends at the summit of the uterine curvature of the TUJ. This asymmetrical development of the glandular mucosa is the cause for the U-shaped excentric slit-like lumen of the TRP in cross-sections; at the antimesometrial side, the thick glandular mucosa projects as a central tissue




Fig. 1. Overall view of the bovine tubouterine junction and adjacent structures. *a* Terminal tubal segment; *b* transition region proper (TRP); *c* uterine apex; *d* ampullary portion of the oviduct; *e* infundibulum; *f* mesometrium; *g* mesosalpinx; *h* infundibulocornual ligament; *white arrow* tubal curvature; *black arrow* uterine curvature. × 0.8

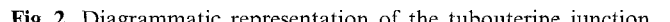


Fig. 2. Diagrammatic representation of the tubouterine junction. *Black lines* Histological borders between the terminal tubal segment (*a*), TRP (*b*) and uterine apex (*c*). Note the asymmetrical distribution of glands in the TRP, and the formation of a mucosal pad (*d*) at the antimesometrial side. *e* Myometrium-myosalpinx; *arrow* concavity of uterine curvature

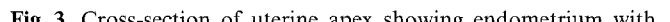


Fig. 3. Cross-section of uterine apex showing endometrium with glandular end-pieces (*a*). The inner circular to spiral layer of myometrium (*b*) is separated from the outer longitudinal layer (*c*) by larger uterine vessels. Estrus, Masson-Goldner. × 56


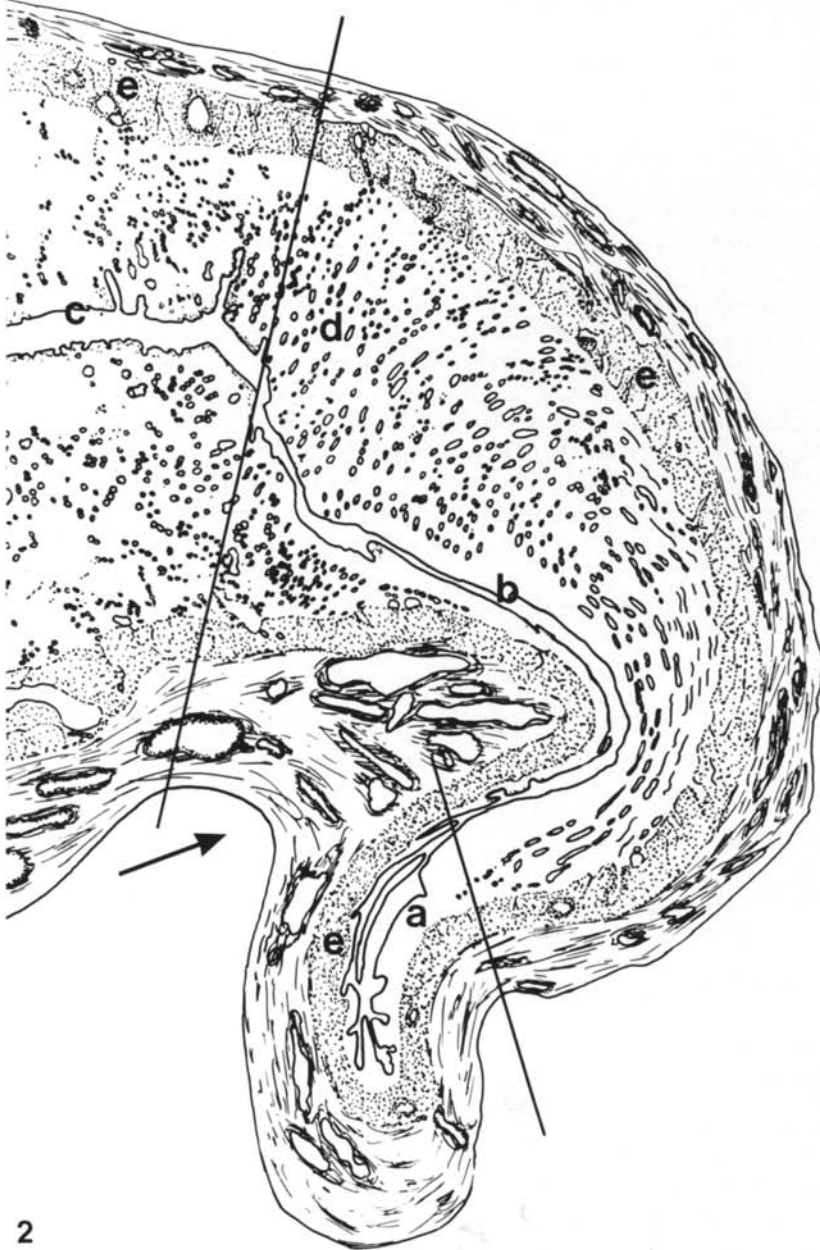
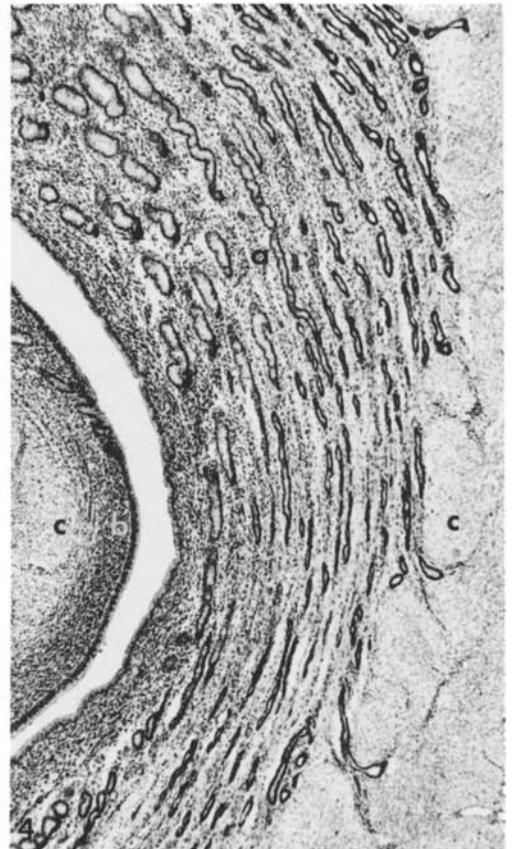
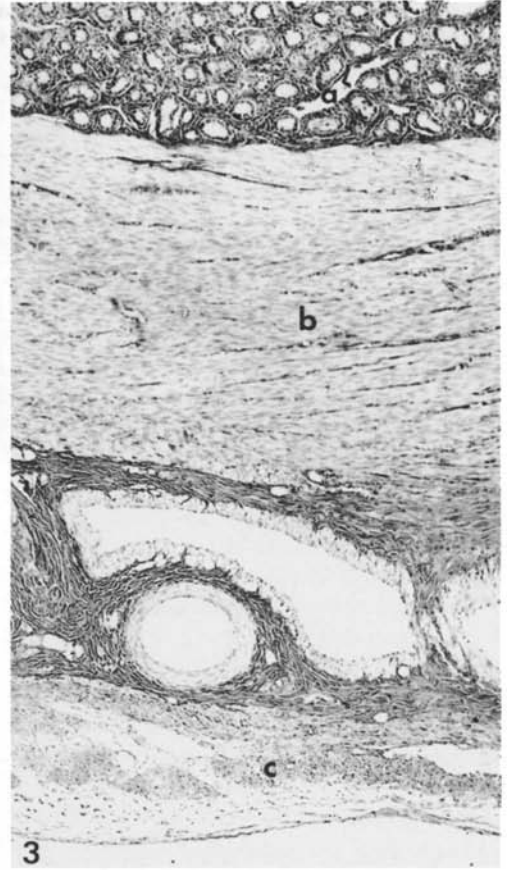
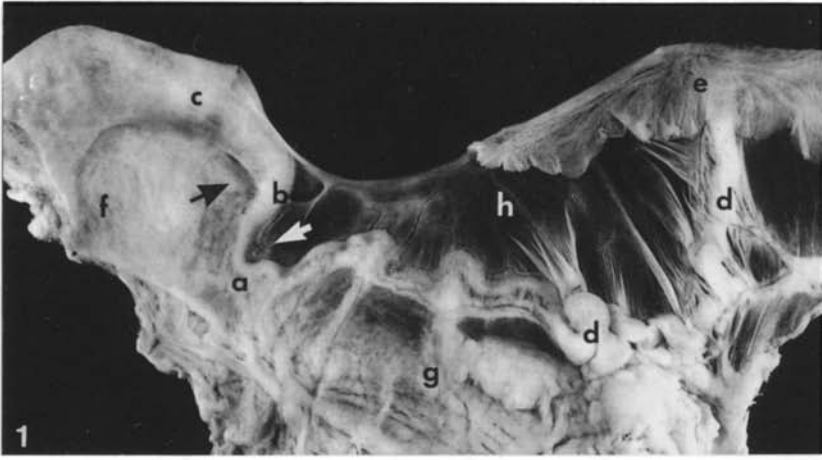


Fig. 4. Longitudinal section of TRP displaying the slit-like lumen at the level of the uterine curvature (similar orientation as in Fig. 2). The first uterine glands are arranged parallel to the lumen and are situated in the mucosal pad (*a*) at the antimesometrial side. *b* Thin mucosa at the mesometrial side; *c* circular layer of myometrium. Proestrus, Masson-Goldner. × 35



pad (Figs. 2, 6, 16). The primary longitudinal folds of the terminal tubal segment start to diverge at the beginning of the TRP. The mesosalpingeal and lateral primary longitudinal folds may fuse, traverse the whole length of the TRP, and terminate at the first transversal ridges of the apical uterine horn. The 1–2 antimesosalpingeal primary longitudinal folds are shorter and terminate at the tubal pole of the mucosal pad mentioned above (Fig. 16). The diverging primary longitudinal folds broaden and flatten before they end. As in the terminal tubal segment, secondary folds and ridges between the primary longitudinal folds of the TRP separate particularly deep well-developed outpocketings with occasional crypts. The convex tissue pad at the antimesometrial side of the TRP generally has a smooth surface (Fig. 16), but may also be contoured by some shallow outpocketings and transversal ridges. On the uterine side of the TRP, the first openings of the true uterine glands may be observed on the surface of the tissue pad and between the broadened terminations of the mesometrial and lateral primary longitudinal folds (Fig. 16).

The uterine apex (Figs. 2, 7) is the third part of the tubouterine transitional region and extends as far as the first uterine caruncles. The star-shaped lumen again lies centrally, whereas the mucosal layer forms low transversal ridges. The openings of the uterine glands, seen in this region, differ slightly in diameter and are mostly situated in the furrows separating the transversal ridges. The openings are situated either on the same level as the surface epithelium or at the top of a small circular elevation. Whereas the long axes of the first uterine glands in the narrow mucosal layer of the TRP run nearly parallel to the luminal surface (Fig. 4), the axes of the glands in the apical uterine portion are more and more radially arranged. Since the length of the glands remains the same, the endometrial mucosa gradually increases in thickness (Fig. 2).

The epithelial surface of the bovine TUJ

The complete TUJ is lined by a simple columnar epithelium containing ciliated and non-ciliated cells. In the terminal tubal segment where the cilia are particularly numerous, ciliated and non-ciliated cells are arranged almost alternately (Figs. 21, 22) on the surface of the primary and secondary folds but, because of their broader shape, ciliated cells dominate the SEM micrographs. In the TRP, the number of ciliated cells decreases slightly; both cell types no longer alternate so regularly, but tend to assemble in groups of 2–4 cells of the same type (Fig. 23). The sides and bottom of the lateral outpocketings and the cryptal linings in the terminal tubal segment and the TRP are virtually devoid of ciliated cells during interestrus and proestrus (Figs. 14, 15). During estrus and postestrus, however, ciliated cells also dominate here (Figs. 11–13).

The non-ciliated cells of the terminal tubal segment and TRP are narrow with slightly bulging luminal apices and short microvilli. They display no cyclical changes, when observed with the SEM.

The epithelial lining of the TRP with its many ciliated cells and the typical uterine surface with only occasional ciliated cells merge in an extremely variable manner (Figs. 17, 18). Principally, the number of ciliated cells in this border region is greater during estrus and postestrus (Figs. 17, 19), compared with interestrus and proestrus (Figs. 18, 20). During the two former phases of the cycle, the epithelial border shifts beyond the TRP into the confines of the uterine horn; moreover, the typical uterine surface epithelium contains more ciliated cells than during interestrus and proestrus. Thus, a clear-cut border between the two epithelial regions is not discernible during estrus and postestrus (Fig. 17). However, in interestrus and proestrus where the heavily ciliated epithelium of the TRP has retracted to the level of the mucosal pad, the borderline to the now virtually non-ciliated uterine epithelial surface runs an intricate course with many projections from either side (Fig. 18). Furthermore, small islands covered with typical uterine epithelium are seen in the confines of the TRP and vice versa. Interestingly, the openings of the uterine glands are regularly surrounded by a small area of non-ciliated uterine surface epithelium (Figs. 19, 20), even when the glands empty at the level of the TRP.

Seen with the SEM, the non-ciliated surface cells at the tip of the uterine horn show a considerable variability in all phases of the cycle (Figs. 24–26). This variability concerns the size of the cells (broad, narrow) and the number of microvilli (few to many). Furthermore, some cells slightly protrude into the lumen. The microvilli are covered and interconnected by a well-developed glycocalyx particularly during interestrus. A characteristic surface pattern is observed during proestrus (Figs. 25–27). In addition to the cellular heterogeneity mentioned above, large spherical epithelial protrusions are very


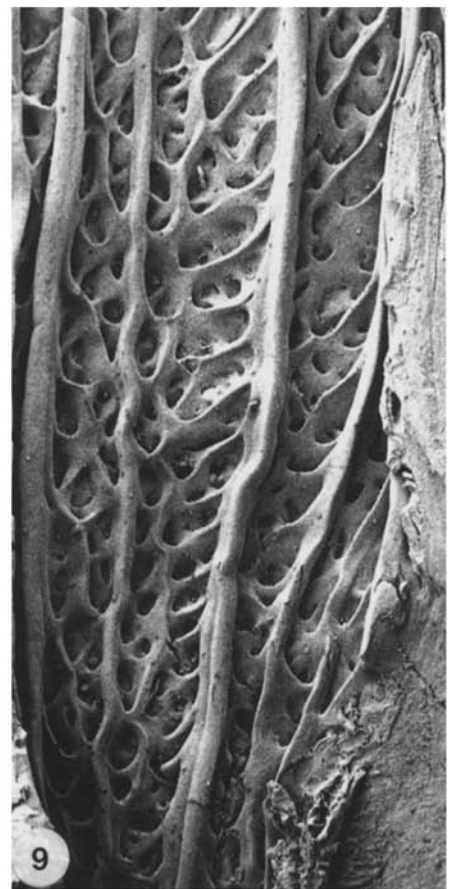
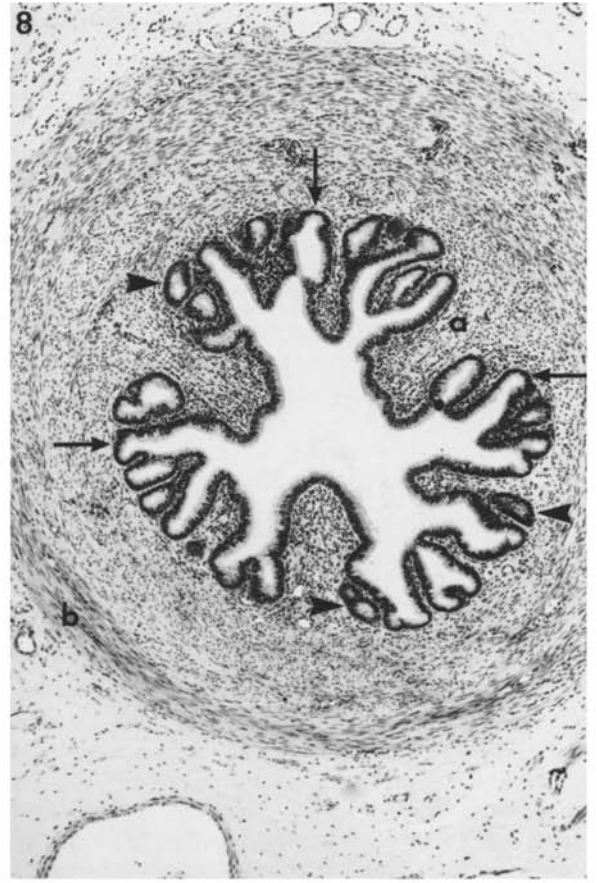
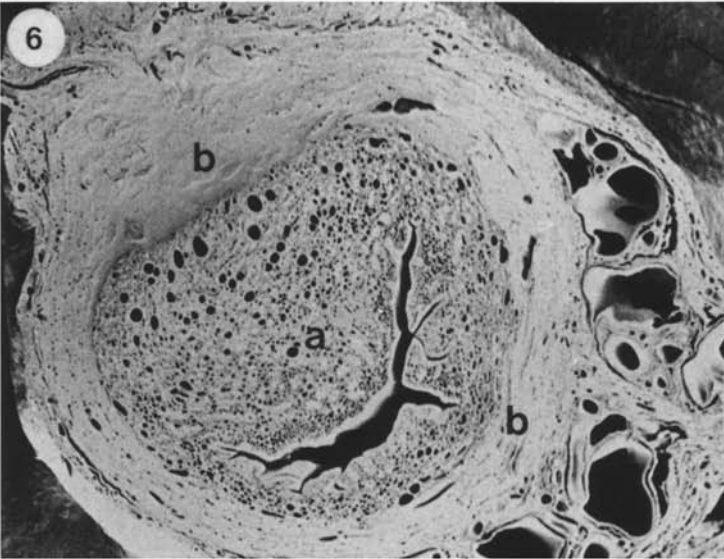
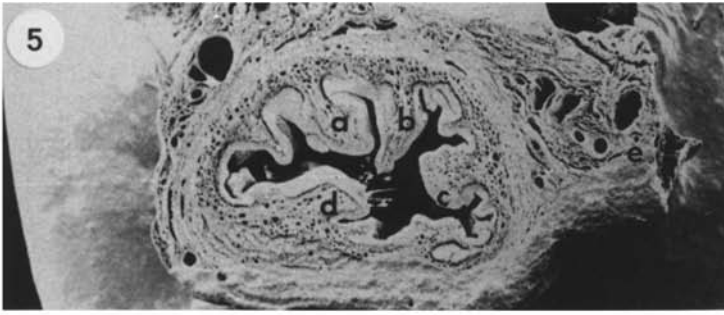
 **Fig. 5.** Cross-section of the terminal tubal segment showing the central lumen and primary longitudinal folds (*a–d*). *e* Mesosalpinx. SEM, proestrus. $\times 21$

Fig. 6. Cross-section of TRP. The asymmetrical slit-like U-shaped lumen has shifted to the mesometrial side and is bordered, on the antimesometrial side, by the thick mucosal pad (*a*), *b* Myometrium. SEM, proestrus. $\times 21$

Fig. 7. Section at the level of the uterine apex. The lumen again has a central position. Note the well-developed vascular layer separating the inner circular and outer longitudinal myometrial musculature. *a* Insertion of infundibulocornual ligament. SEM, proestrus. $\times 21$

Fig. 8. Cross-section of the terminal tubal segment displaying primary and secondary longitudinal folds. The system of lateral luminal outpocketings is visible (*arrows*) beneath and between the mucosal folds. Cross-sections of their blind, adovarially pointing ends appear as closed epithelial rings (*arrowheads*). The thick inner longitudinal (*a*) and intermediate circular (*b*) muscular layers are also indicated. A continuous outer longitudinal layer is not yet present. Estrus, Masson-Goldner. $\times 56$

Fig. 9. Surface morphology of the terminal tubal segment, opened longitudinally. The system of short slipper-shaped lateral outpocketings is visible between the parallel-running longitudinal folds. The blind ends of the pockets point to the adovarial side (*bottom*). SEM, postestrus. $\times 28$



prominent in circumscribed areas. Protrusions (Fig. 25) are normally smooth-contoured and without microvilli, and are connected to the parent cell by slender stalks. When these are severed, a considerable portion of the cell is pinched off into the lumen. In other areas, the stalks are not severed but the protrusions collapse, leaving behind crater-like indentations of the apical cell surface. Another characteristic of the uterine surface in proestrus and estrus is the occurrence of circumscribed epithelial lesions with exposure of the basal lamina, following the complete shedding of a group of cells (Fig. 26). Prior to shedding, fluid is accumulated between the basal lamina and the intercellular spaces, giving rise to intraepithelial vesicles and cysts (Fig. 27).

In all phases of the cycle, the tubouterine surface is covered by varying amounts of a mucous secretion that tends to agglomerate the cilia and microvilli (Figs. 28–30).

Vascularization pattern of the bovine TUJ

The microvascularization pattern of the mucosa differs within the three regions of the tubouterine junction.

In the uterine apex, highly coiled spiral arteries traverse the basal two thirds of the endometrium parallel to the uterine glands. In the luminal third of the endometrium, these arteries split up into a number of smaller vessels and form a unilayered capillary network around the glands and a two- to three-layered network below the surface epithelium (Fig. 33).

In the TRP (Figs. 29–32), larger longitudinal arteries are located at the bases of the broadening primary longitudinal folds. From here, a close-set series of smaller arteries is observed ascending in the center of the folds. Together with their branches, capillaries and venules, these ascending arteries build up a multilayered vascular plexus within the mucosa (Figs. 29–31). The vascular density in the folds suggests the presence of an erectile tissue. A similar dense vascularization is observed below the surface of the mucosal pad in the TRP (Fig. 32).

Although the longitudinal folds of the TRP are in continuation with those of the terminal tubal segment, the vascularization within the folds is drastically reduced here (Fig. 28). In the tube, larger longitudinal vessels in the inner longitudinal musculature give rise to a loosely arranged unilayered subepithelial capillary network.

Distribution of musculature in the bovine TUJ

The musculature of the terminal tubal segment (Fig. 8) may be divided into an inner longitudinal layer that is particularly well developed in the bases of the primary longitudinal folds, an intermediate spiral or circular layer that represents the bulk of the musculature, and an incomplete outer system of isolated bundles with a predominantly longitudinal orientation. This outer longitudinal musculature is intermingled with subserosal muscle bundles of varying directions. Toward the uterus, the outer longitudinal bundles increase in thickness and

converge, so that they form a complete layer at the level of the uterine apex (Fig. 3).

The intermediate spiral to circular layer increases through the TRP and uterine apex. The inner longitudinal layer of the terminal tubal segment, however, fades gradually in an uterine direction. At the tip of the horn, only single isolated longitudinal strands are occasionally seen below the endometrium. As a rule, the distal endings of the uterine glands border on the innermost spiral or circular bundles (Fig. 3), or are even embedded into them.

A separate muscular sphincter at the level of the bovine TUJ is not observed.

Discussion

Our gross anatomical observations support the earlier descriptions by Andersen (1928), Hook and Hafez (1968), Beck and Boots (1974), indicating that the narrow terminal segment of the Fallopian tube thickens continuously at the level of the TRP and the apex uteri; furthermore, the bovine tubouterine transition follows a typical sigmoidal course. We have distinguished two curvatures: a tubal curvature with an antimesosalpingeal concavity and uterine curvature with its concavity at the mesometrial side. Both curvatures are arranged in the same plane only exceptionally. As a rule they overlap partially in a spiral-like fashion. The infundibulocornual ligament is attached to the tubal curvature, preferably to its antimesosalpingeal side. This ligamentous fold contains bundles of longitudinally arranged musculature. Hook and Hafez (1968) speculate that contractions of the intraligamentous musculature may regulate variations in the degree of flexure of the TUJ during the estrus cycle. Schilling (1962), on the other hand, concludes from his observations, that the infundibulocornual ligament is related to the process of ovum-pick-up.

Lumen and surface contours of the bovine TUJ are more complicated than hitherto recognized. In the terminal tubal segment, the lumen is contoured by 4–8 regularly distributed primary longitudinal folds and a


 **Fig. 10.** Subepithelial outpocketings in the terminal tubal segment give the erroneous impression of oviductal glands. Estrus, Masson-Goldner. $\times 140$

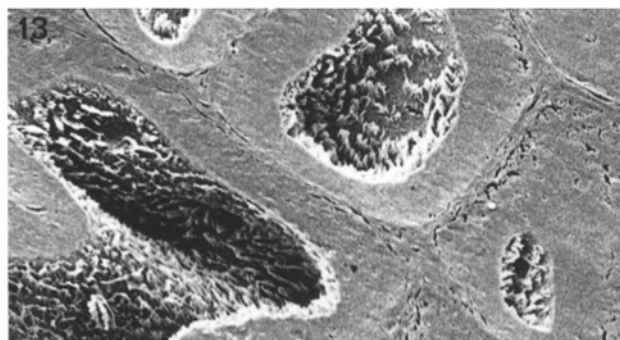
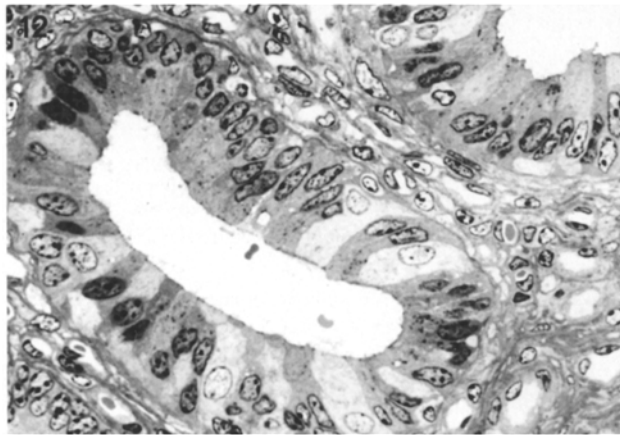
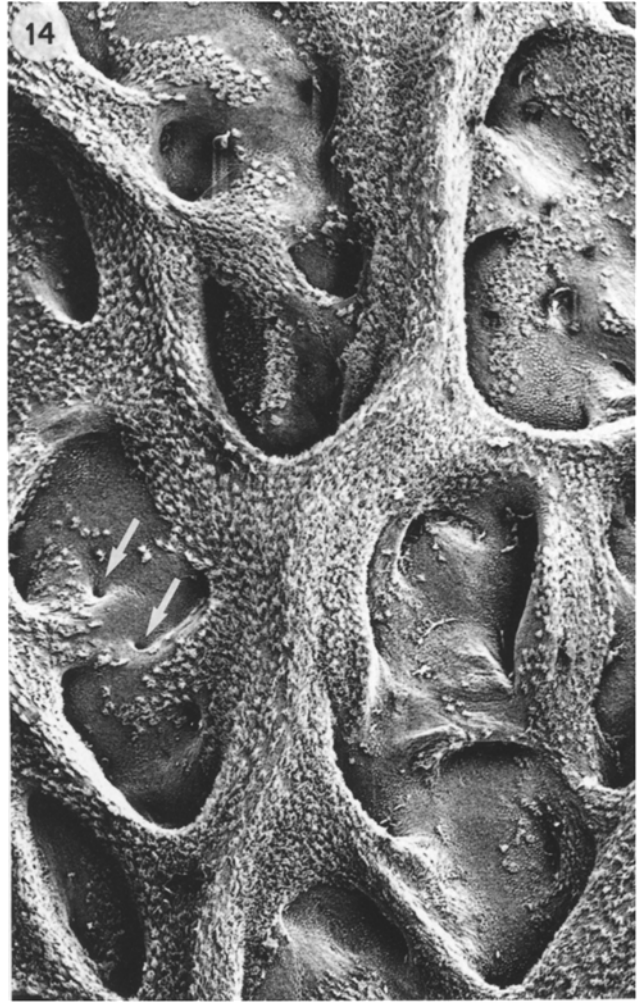
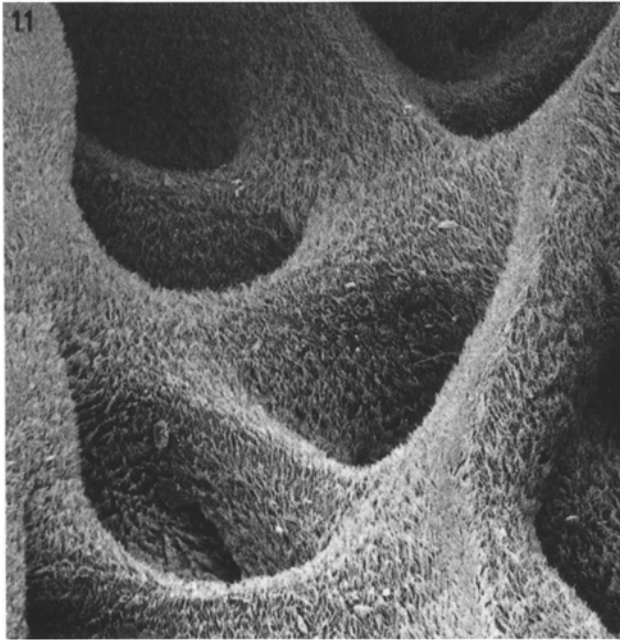
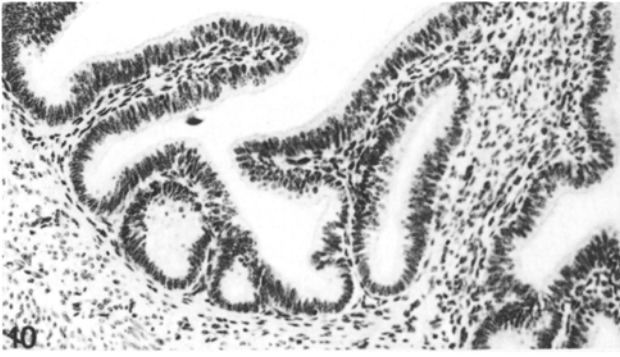
Fig. 11. The sides and bottom of lateral luminal outpocketings are covered by an epithelium with many ciliated cells during estrus and postestrus. SEM, postestrus. $\times 280$

Fig. 12. Cross-section of a luminal outpocketing in estrus showing an abundance of ciliated cells (*light cells*). Semithin section. $\times 350$

Fig. 13. Blind ends of luminal outpocketings with many ciliated cells. SEM, postestrus. $\times 280$

Fig. 14. The sides and bottom of outpocketings are virtually devoid of ciliated cells in pro- and interestrus, exposing the entrances of short tubouterine crypts (*arrows*). SEM, interestrus. $\times 140$

Fig. 15. The side and bottom (*a*) of an outpocketing in interestrus are lined by a non-ciliated epithelium. *Arrows* Entrances of tubouterine crypts. Semithin section. $\times 350$



number of secondary folds, ridges and chords. A system of shallow outpocketings with their blind ends pointing to the ovarian side is present between these mucosal projections. The openings of short tubulo-alveolar crypts lie at the bottom of the outpocketings. These crypts have been misinterpreted as continuations of uterine glands extending into the oviduct (Lombard et al. 1950; Hafez and Black 1969; Hunter et al. 1991). The last true uterine glands, according to our observations, terminate in the uterine half of the TRP.

In the TRP, the lumen narrows to a slit with a U-shaped diameter on cross-sections. This conformation is caused by the existence of a smooth-surfaced mucosal pad lying at the antimesometrial side. The primary longitudinal folds of the terminal tubal segment broaden and diverge when they reach the level of the TRP. The anti-mesosalpingeal set of primary folds terminates at the tubal end of the mucosal pad, whereas the mesosalpingeal and lateral folds reach the level of the uterine apex. Outpocketings and occasional crypts, as described for the terminal tubal segment, are also observed in the TRP. Interestingly, the mucosa in the broadening longitudinal folds and in the pad of the TRP is heavily vascularized, giving the appearance of an erectile tissue. Thus, the notion of Andersen (1928) and Hook and Hafez (1968) that specialized mucosal structures are lacking in the bovine TUJ is not substantiated by our study. This region of heavily vascularized mucosal pad and folds may be the functional equivalent to the papillae described in the TUJ of other mammals (Hafez and Black 1969; Beck and Boots 1974).

No caruncles are present in the uterine apex. The openings of the uterine glands are positioned in the depressions between the shallow transversal folds of the region, and thus seem to be arranged in irregular rows, as has been noted by Vollmerhaus (1960).

Our findings concerning the arrangements of musculature in the TUJ corroborate the descriptions given by Schilling (1962). A separate sphincter, as in other mammals (Beck and Boots 1974), is lacking in the bovine TUJ. Nevertheless, a blocking mechanism is present in the bovine, preventing the escape of tubal fluid into the uterus during estrus and until about 72 h after ovulation (Black and Davis 1962). Insufflation experiments by Black and Davis (1962) indicate that the musculature of the 3–4 cm of tubal isthmus preceding the TUJ is responsible for this effect.

The surface epithelium of the bovine TUJ consists of a single layer with ciliated and non-ciliated cells. The degree of ciliation is higher during estrus and postestrus than during interestrus and proestrus. This trend is documented by the following observations: (1) the lateral outpocketings and the short crypts in the terminal tubal segment and the TRP are virtually devoid of ciliated cells during inter- and proestrus, but are dominated by ciliated cells during estrus and postestrus. (2) The borderline between the heavily ciliated epithelium of the TRP and the sparsely ciliated uterine surface epithelium is translocated in a uterine direction in estrus and postestrus and shifts back to a tubal direction during inter- and proestrus. (3) Ciliated cells, occurring single or in

small groups, increase in number in the characteristic surface epithelium of the uterine apex during estrus and postestrus. In contrast to the pig, where Sidler et al. (1986) have observed a concentration of ciliated cells around the mouths of the uterine glands, the immediate surroundings of the bovine glandular openings are generally devoid of ciliated cells. The considerable cyclic ciliation and deciliation in the TUJ is the first description of a ciliated cell cycle in this region of the female bovine urogenital tract, but corresponds well with data obtained from the Fallopian tubes of a number of species, indicating increased ciliogenesis under the influence of estradiol, and deciliation under the influence of elevated levels of serum progesterone (Verhage et al. 1973, 1979; Seki et al. 1978; Odor et al. 1980; Donnez et al. 1985). Bajpai et al. (1980) have shown that tubal non-ciliated cells have the ability to transform into ciliated cells following estradiol treatment.

SEM inspection of the apical surface of the non-ciliated cells in the uterine apex reveals considerable variability




Fig. 16. Surface morphology of TRP, opened longitudinally from the mesometrial side. Note the diverging primary longitudinal folds and particularly the deep outpocketings between them. The mesometrial folds (*a, b*) extend further in an aduterine direction than the antimesometrial folds (*c, d*), which end on the border of the smooth-surfaced mucosal pad (*e*). Arrows Openings of the first true uterine glands. SEM, estrus. $\times 28$

Fig. 17. During estrus and postestrus, ciliated cells increase in the epithelium of the uterine apex. Furthermore, the richly ciliated epithelium of the TRP extends farther in an aduterine direction. Thus, no clear-cut borderline is visible between the uterine surface epithelium (*a*) and that of the TRP (*b*). Arrows Glandular openings. SEM, estrus, $\times 28$

Fig. 18. During inter- and proestrus a clear-cut tortuous borderline is visible between the epithelia of the uterine apex (*a* devoid of ciliated cells) and TRP (*b* heavily ciliated). Arrows Uterine glands. SEM, interestrus. $\times 28$

Fig. 19. Surface epithelium of the uterine apex in postestrus with many ciliated cells. Note that the area around the glandular openings (arrows) is generally free of ciliated cells. SEM. $\times 140$

Fig. 20. The surface epithelium of the uterine apex in interestrus is virtually devoid of ciliated cells (compare with Fig. 19). Two glandular openings are also seen. SEM. $\times 280$

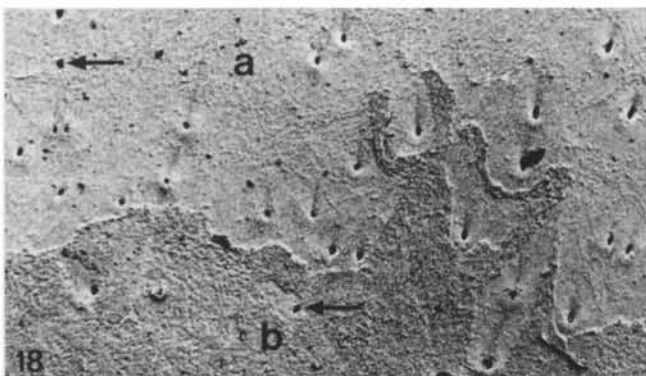
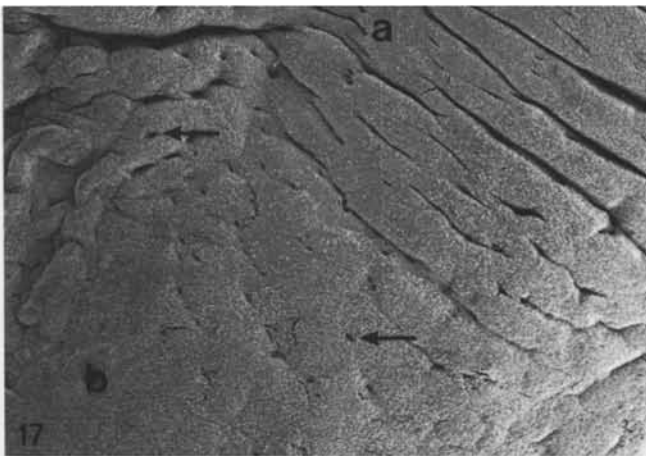
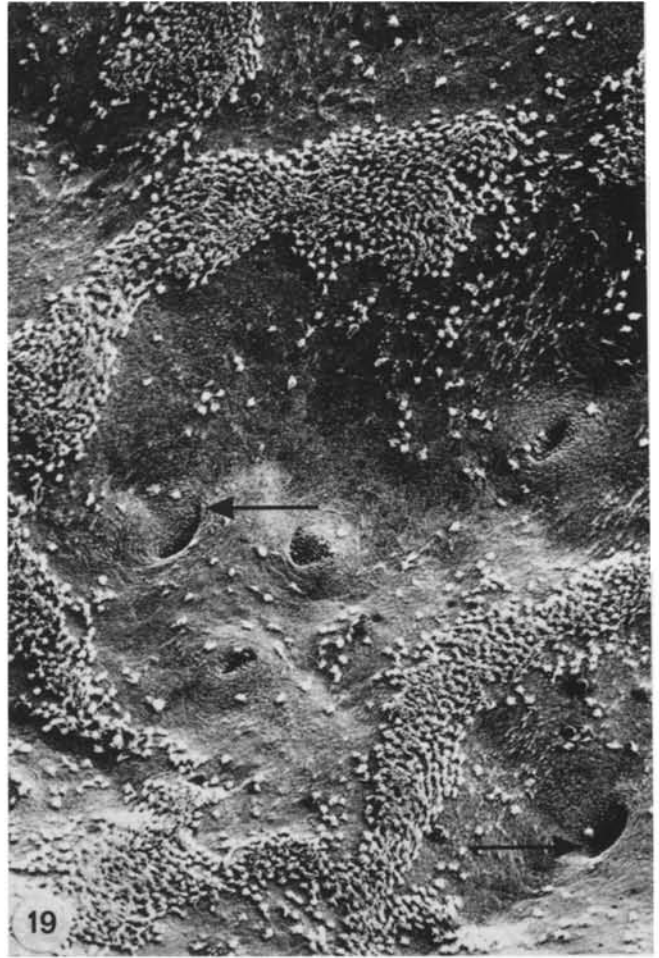
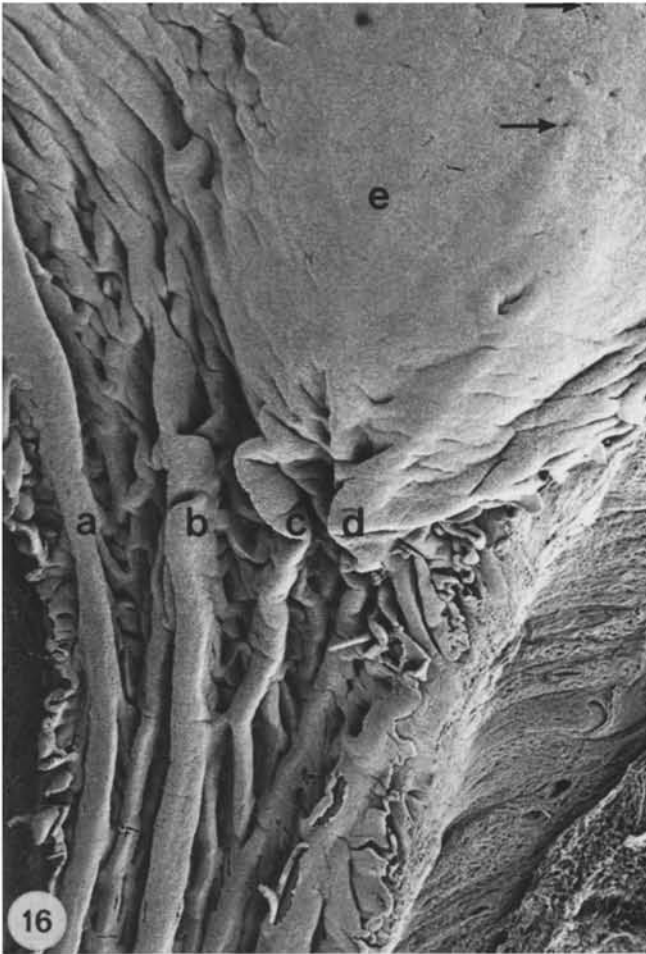
Fig. 21. Ciliated and non-ciliated cells alternate regularly on the folds of the terminal tubal segment (compare with Figs. 23, 24). The non-ciliated cells display short microvilli. SEM, interestrus. $\times 2800$

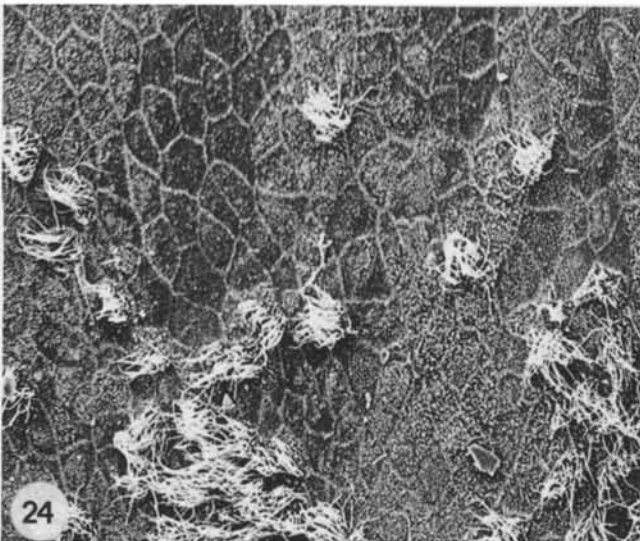
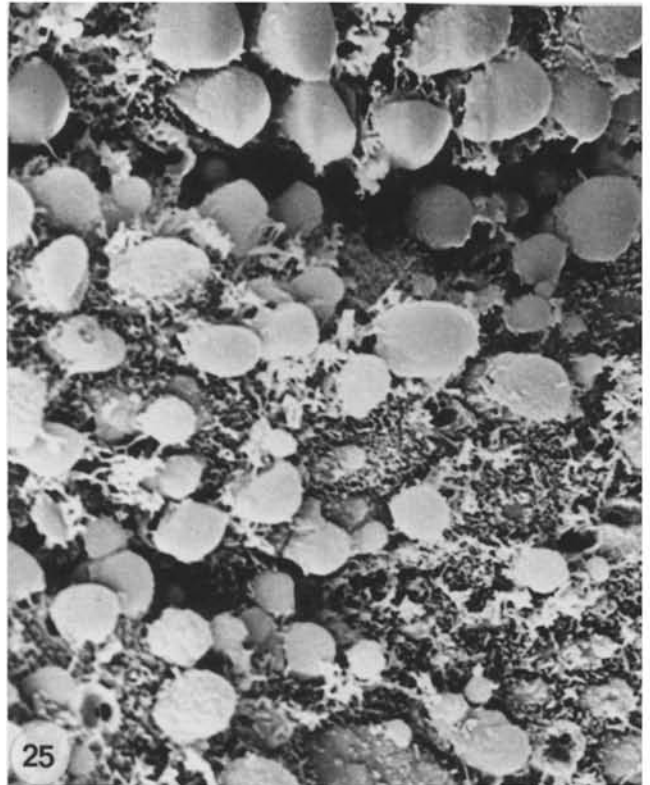
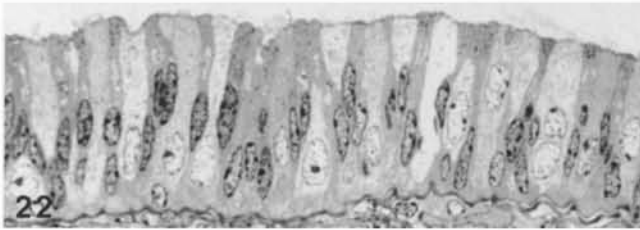
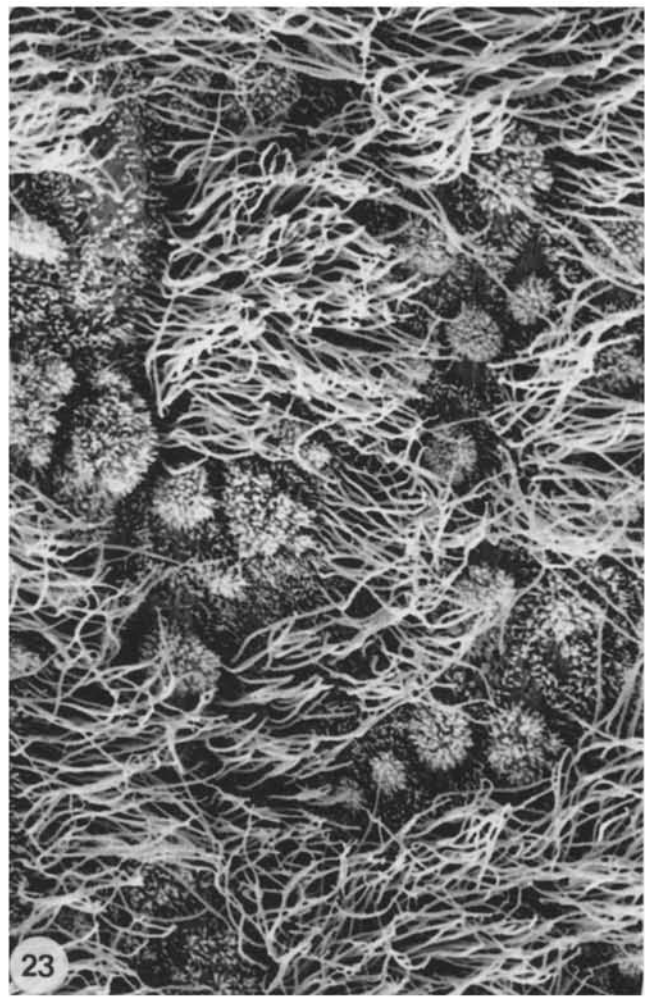
Fig. 22. Characteristic simple columnar tubal surface epithelium containing slender non-ciliated (*dark*) cells and broader ciliated (*light*) cells in a regular arrangement. Semithin section, estrus. $\times 560$

Fig. 23. In the TRP, groups of ciliated cells are situated between groups of non-ciliated cells. The latter protrude slightly into the lumen. SEM, interestrus. $\times 2800$

Fig. 24. The non-ciliated cells in the uterine apex vary in size, shape, number and length of microvilli. SEM, postestrus. $\times 700$

Fig. 25. During proestrus, groups of non-ciliated cells in the uterine apex display smooth-surfaced, bulbous apical protrusions. SEM. $\times 2800$





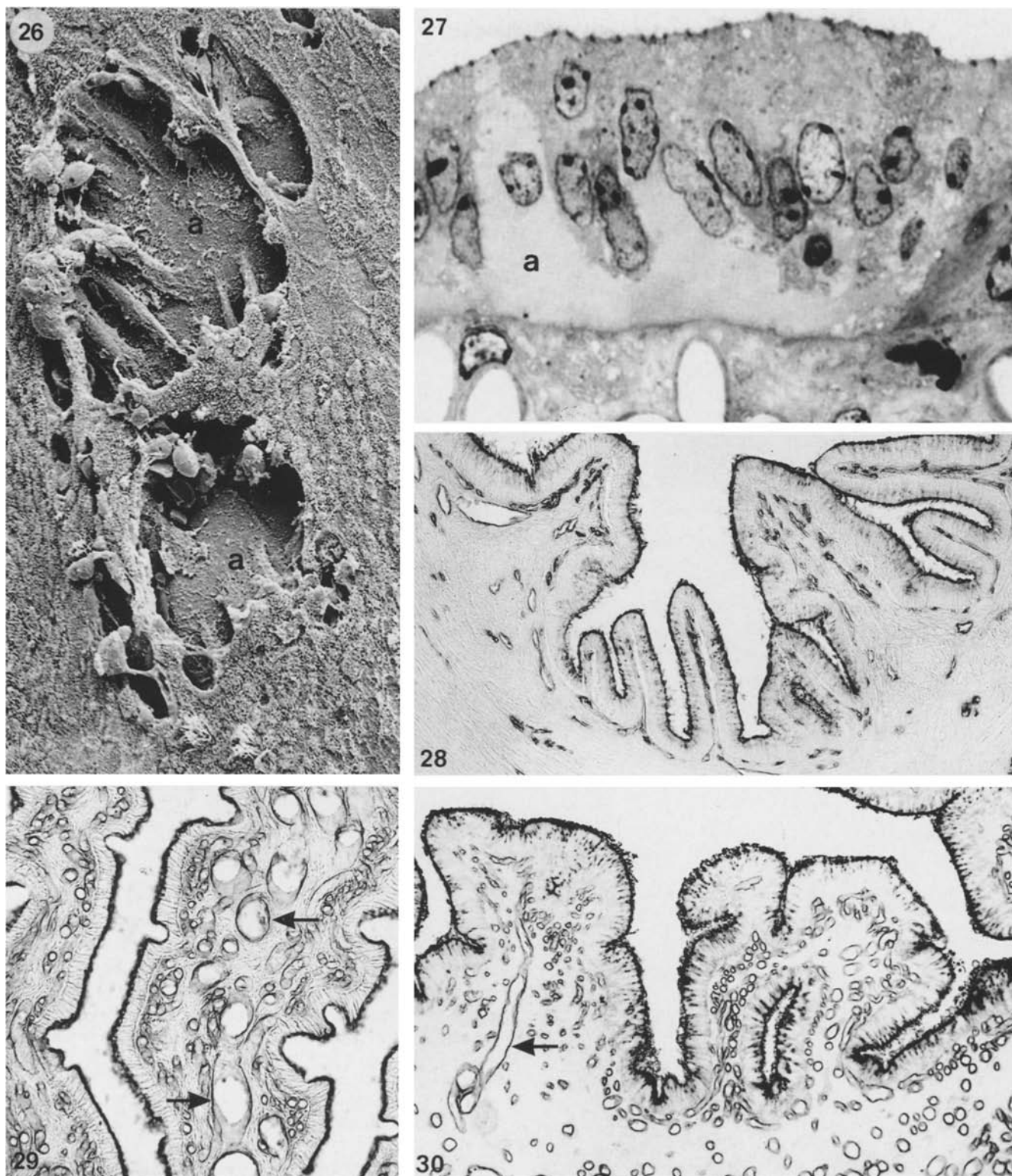
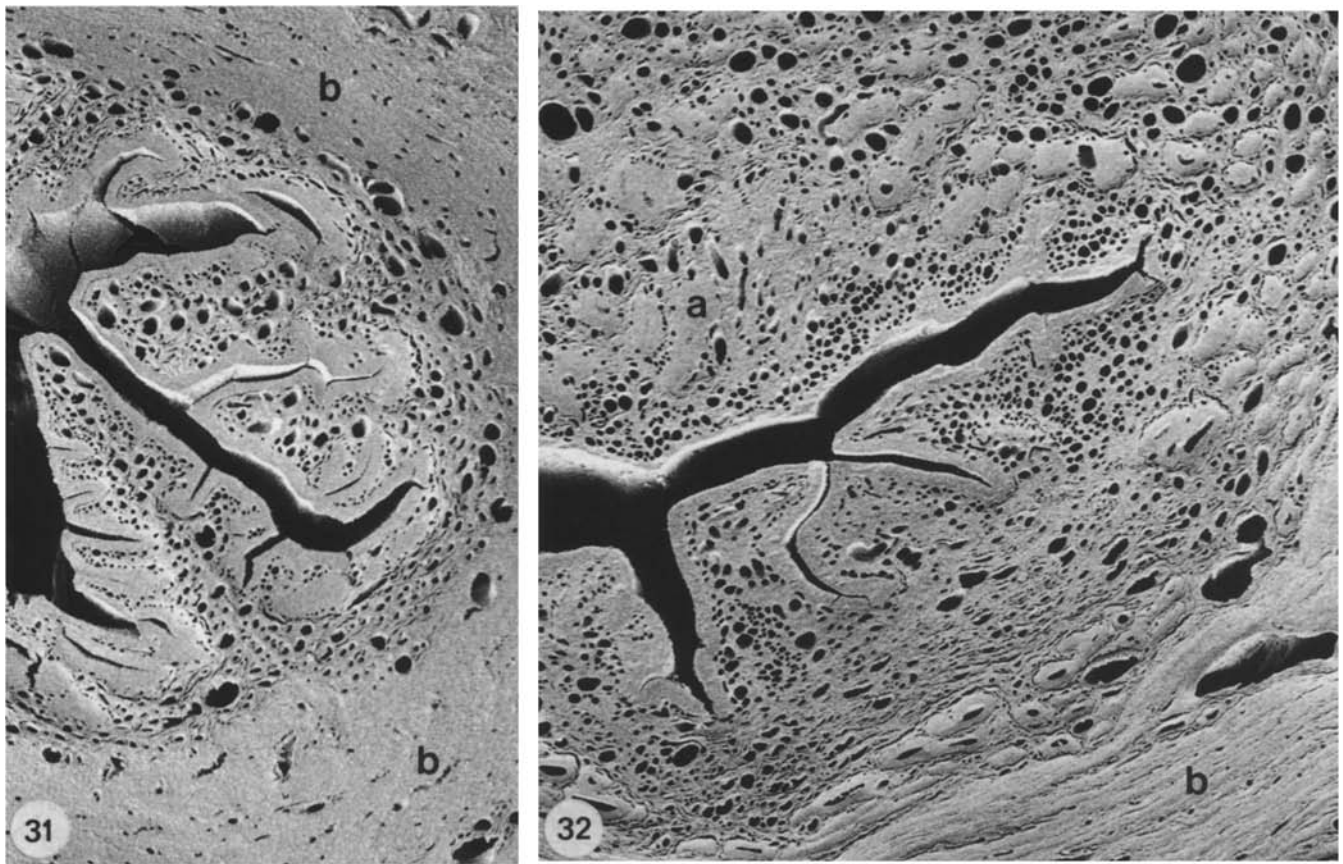


Fig. 26. Circumscribed epithelial lesions, exposing the basal lamina (*a*) are a manifestation of rapid cell loss in the uterine surface epithelium during proestrus. SEM. $\times 700$

Fig. 27. Intraepithelial fluid accumulation (*a*) precedes desquamation as demonstrated in Fig. 26. Semithin section, proestrus. $\times 1400$

Figs. 28–30. GS I lectin histochemistry demonstrates glycocalyx and vascular endothelial basal lamina. Interestrus. $\times 140$. **Fig. 28.** Moderate mucosal vascularization in the terminal tubal segment.

Fig. 29. Longitudinal section through the base of a primary fold in the heavily vascularized TRP. Note the close-set series of central ascending vessels (*arrows*) and the increasing subepithelial microvascularization. **Fig. 30.** Cross-section of heavily vascularized, diverging, longitudinal folds in the TRP. *Arrow A* central ascending vessel (compare with Fig. 29).



Figs. 31, 32. Cross-section of TRP: diverging longitudinal folds in **Figs. 31, 32** and mucosal pad (*a*) flanking the slit-like lumen in **Fig. 32** are supplied by a dense vascular plexus, as clearly demonstrated in these perfused specimens. The myometrium (*b*) is less densely vascularized. SEM, proestrus. $\times 70$

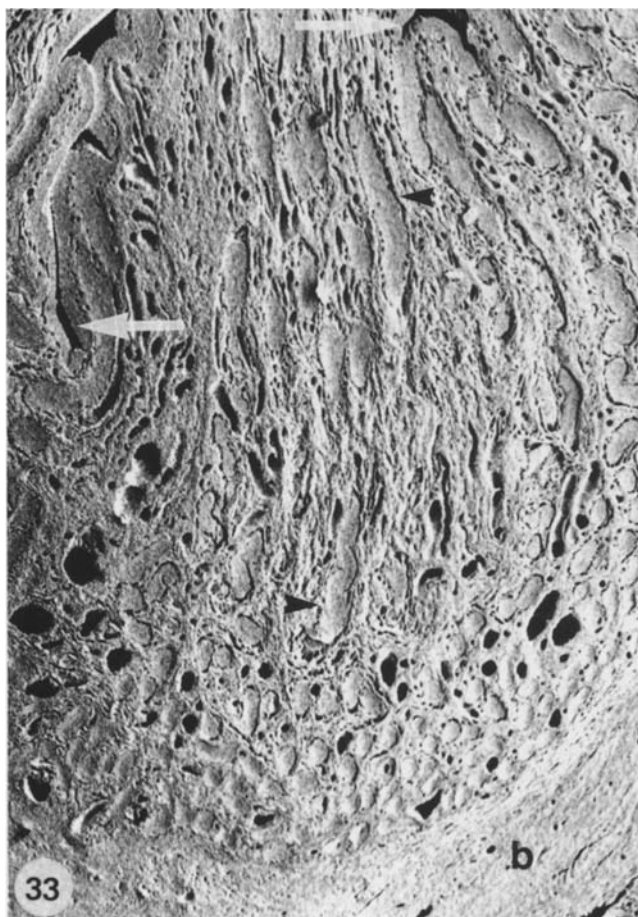


Fig. 33. Compared with **Figs. 31, 32** (TRP), the endometrial vascularization in the uterine apex is distinctly reduced. *White arrows* Uterine lumen; *arrowheads* uterine glands; *b* myometrium. SEM, proestrus. $\times 70$

ty concerning the size, shape, number and length of microvilli during all phases of the estrus cycle. During proestrus, groups of cells present prominent bulbous apical protrusions. Protrusions generally have smooth surfaces and are connected by slender stalks to the parent cell. When the stalks are severed, a considerable portion of the cytoplasm is pinched off into the lumen. We interpret these protrusions as signs of cellular turnover rather than an apocrine type of secretion (Nilsson 1972; Aitken 1975). Another fate of the protrusions that we have also observed, is described by Guillomot and Guay (1982) as occurring by day 18–21 of the bovine uterine cycle: viz., the collapse of the protrusions resulting in craters between the cells. As a further sign of epithelial degeneration during proestrus and estrus, we have observed circumscribed lesions exposing the underlying basal lamina. This process of partial desquamation seems to be initiated by fluid accumulation and the occurrence of cysts in the epithelium.

Acknowledgements. The authors appreciate the valuable technical help of Mrs. K. Dassler, Mrs. M. Schimmel, Mrs. E. Stauber and Mr. O. Siegert. Special thanks are extended to Mr. K.H. Kessler for providing the line diagram and to Dr. Cheryl Lang for her assistance in the English translation of the manuscript. This work was supported by DFG grant Wr 7/7-1.

References

- Aitken RJ (1975) Ultrastructure of the blastocyst and endometrium of the roe deer (*Capreolus capreolus*) during delayed implantation. *J Anat* 119:369–384
- Andersen DH (1928) Comparative anatomy of the tubo-uterine junction. *Histology and physiology in the sow. Am J Anat* 42:255–290
- Anderson TF (1951) Techniques for the preservation of three-dimensional structure in preparing specimens for the electron microscope. *Trans NY Acad Sci* 13:130–134
- Bajpai VK, Pathak RK, Shipstone AC, Harper MJK, Herbert DC (1980) Does interconversion occur in tubal epithelium? *Anat Rec* 196:12A–13A
- Beck RL, Boots RL (1974) The comparative anatomy, histology and morphology of the mammalian oviduct. In: Johnson AD, Foley CW (eds) *The oviduct and its function*. Academic Press, New York London, pp 1–51
- Black DL, Davis J (1962) A blocking mechanism in the cow oviduct. *J Reprod Fertil* 4:21–26
- Donnez J, Casanas-Roux F, Caprasse J, Ferin J, Thomas K (1985) Cyclic changes in ciliation, cell height, and mitotic activity in human tubal epithelium during reproductive life. *Fertil Steril* 43:554–559
- Ertl C, Wrobel KH (1992) Distribution of sugar residues in the bovine testis during postnatal ontogenesis demonstrated with lectin-horseradish peroxidase conjugates. *Histochemistry* 97:161–171
- Forssmann WG, Ito S, Weihe E, Aoki A, Dym M, Fawcett DW (1977) An improved perfusion fixation method for the testis. *Anat Rec* 188:307–314
- Grunert E (1982) Sexualzyklus. In: Grunert E, Berchthold M (eds) *Fertilitätsstörungen beim weiblichen Rind*. Parey, Berlin Hamburg, pp 52–63
- Guillomot M, Guay P (1982) Ultrastructural features of the cell surfaces of uterine and trophoblastic epithelia during embryo attachment in the cow. *Anat Rec* 204:315–322
- Hafez ESE, Black DL (1969) The mammalian uterotubal junction. In: Hafez ESE, Blandau RJ (eds) *The mammalian oviduct*. University of Chicago Press, Chicago London, pp 53–126
- Hook SJ, Hafez ESE (1968) A comparative anatomical study of the mammalian uterotubal junction. *J Morphol* 125:159–184
- Hunter RHF, Wilmut I (1984) Sperm transport in the cow: periovulatory redistribution of viable cells within the oviduct. *Reprod Nutr Dev* 24:597–608
- Hunter RHF, Fléchon B, Fléchon JE (1991) Distribution, morphology and epithelial interactions of bovine spermatozoa in the oviduct before and after ovulation: a scanning electron microscope study. *Tissue Cell* 23:641–656
- Jerusalem C (1963) Eine kleine Modifikation der Goldner-(Masson)-Trichromfärbung. *Z Wiss Mikrosk* 65:320–321
- Kann ML, Fouquet JP (1977) Bull spermatozoa in the female tract after natural mating. A preliminary ultrastructural study of uterotubal junction. *Ann Biol Anim Biochem Biophys* 17:165–172
- Larsson B, Larsson KC (1986) Sperm localization in the oviducts of artificially inseminated dairy cattle. *Acta Vet Scand* 27:303–312
- Lombard L, Banner BM, McNutt SH (1950) The morphology of the oviduct of virgin heifers in relation to the estrous cycle. *J Morphol* 86:1–15
- Nilsson O (1972) Ultrastructure of the process of secretion in the rat. Uterine epithelium at preimplantation. *J Ultrastruct Res* 40:572–580
- Odor DL, Gaddum-Rosse P, Rummery RE, Blandau RJ (1980) Cyclic variations in the oviductal ciliated cells during the menstrual cycle and after estrogen treatment in the pig-tailed monkey, *Macaca nemestrina*. *Anat Rec* 198:35–37
- Schilling E (1962) Untersuchungen über den Bau und die Arbeitsweise des Eileiters beim Schaf und Rind. *Zentralbl Med Vet* 9:805–853
- Seki K, Rawson J, Eddy CA, Smith NK, Pauerstein CJ (1978) Deciliation in the puerperal Fallopian tube. *Fertil Steril* 29:75–83
- Sidler X, Zimmermann W, Leiser R (1986) Das normale zyklische Geschehen im Endometrium des Schweines. *Eigenverlag Klinik für Nutztiere, Universität Bern*
- Spurr AR (1969) A low-viscosity epoxy resin embedding medium for electron microscopy. *J Ultrastruct Res* 26:31–43
- Verhage HG, Abel JH, Tietz WJ, Barrau MD (1973) Development and maintenance of the oviductal epithelium during the estrous cycle in the bitch. *Biol Reprod* 9:460–474
- Verhage HG, Bareither ML, Jaffe RC, Akbar M (1979) Cyclic changes in ciliation secretion and cell height of the oviductal epithelium in women. *Am J Anat* 156:505–522
- Vollmerhaus B (1960) Zur Morphologie der Uterindrüsen des Rindes. *Berl München Tierärztl Wochenschr* 73:1–5
- Wrobel KH, Sinowatz F, Kugler P (1978) Zur funktionellen Morphologie des Rete testis, der Tubuli recti und der Terminalsegmente der Tubuli seminiferi des geschlechtsreifen Rindes. *Anat Histol Embryol* 7:320–335